Structural Basis for Reaction Mechanism and Drug Delivery System of Chromoprotein Antitumor Antibiotic C-1027

Yasushi Okuno,[†] Takashi Iwashita,[‡] and Yukio Sugiura*,[†]

Contribution from the Institute for Chemical Research, Kyoto University, Uji, Kyoto 611-0011, Japan, Suntory Institute for Bioorganic Research, Wakayamadai, Shimamoto-cho, Mishima-gun, Osaka 618-8503, Japan

Received December 9, 1999

Abstract: Antitumor antibiotic C-1027, which is regarded as a natural model of a drug delivery system, consists of a carrier apoprotein (Apo) and an enediyne chromophore (Chr). We have compared three solution structures of the DNA−Chr complex, Apo−Chr complex, and free Chr determined by high-resolution NMR experiments. The guest molecule, C-1027 chromophore, showed two distinct binding modes fitted to binding sites of the hosts (target DNA and carrier Apo). The novel Chr interacts with DNA through its benzoxazolinate and aminosugar moieties, and also with Apo through the benzoxazolinate and macrocyclic moieties. The superposition of Chrs in these three states clearly revealed conformational deviation of the 16-membered macrocyclic moiety containing an intra-chlorophenol ring. Ab initio calculations supported good correlation between the reactivity and the conformational alteration of Chr induced in the hosts. The present results provide a molecular basis and implication for the host-recognition mode, the reaction mechanism, and the drug delivery system of chromoprotein C-1027.

C-1027 is a molecular antitumor antibiotic isolated from *Streptomyces globisporus* C-1027.[1] The chromoprotein C-1027 consists of an apoprotein (Apo) containing 110 amino acids and a labile enediyne chromophore (Chr).[2] The Apo acts as a specific carrier to protect and transport Chr.[3] The Chr is a member of the enediyne family such as neocarzinostatin,[4] esperamicin,[5] calcheamicin,[6] and kedarcidin.[7] Of special interest is the fact that C-1027 Chr is the most labile enediyne among the families in the protein-free state. The reactive enediyne Chr is released from Apo and then comes into contact with the target DNA.[8] This enediyne bound to DNA provides a molecular basis for potential antitumor and DNA-cleaving activities of C-1027.[9] Therefore, the chromoprotein C-1027 can be regarded as a natural model of a drug delivery system (DDS).

As well as other enediyne antibiotics, C-1027 induces the cleavage of duplex DNA by hydrogen abstraction.[10] The preferred cutting sites were found at GTTAT/ATAAC, CTTTT/AAAAG, ATAAT/ATTAT, CTTTA/TAAAG, and CTCTT/AAGAG sequences which consist of five nucleotide sequences with a two-nucleotide 3′-stagger of the cleaved residues (cleaved residues underlined).[11] The most striking characteristic of C1027−Chr is the fact that the DNA cleavage reaction proceeds even in the absence of an activating agent, namely a reductant, in contrast to the other enediyne reactions triggered by thiol. Iida and Hirama reported that the constraint of the nine-membered ring of C1027−Chr may contribute to lowering the barrier for interconversion between the enediyne and biradical forms, and consequently the reaction process becomes reversible at ambient temperature.[12] How C1027−Chr remain inactive in Apo but become active in DNA? In this study, we have investigated not only the recognition mode between the guest drug (C1027−Chr) and its host (target DNA or carrier Apo) but also the conformational changes of C1027−Chr in DNA-bound, Apo-bound, and free states. The reaction mechanism of chromoprotein C-1027 can be elucidated on the basis of the correlation between the structural changes and the activity of Chr. These results provide valuable molecular information about the DDS of C-1027.

Materials and Methods

Materials. Purified C-1027 and the structure coordinates of Chr−Apo complex were kindly supplied by Dr. Otani (Taiho, Tokushima) and Dr. Ishiguro,[13] respectively. A stable aromatized form of C1027−

* Corresponding author: Yukio Sugiura, Institute for Chemical Research, Kyoto University, Uji, Kyoto 611-0011, Japan. Telephone: 81-774-38-3210. Fax: 81-774-32-3038. E-mail: sugiura@scl.kyoto-u.ac.jp.

[†] Kyoto University.

[‡] Suntory Institute for Bioorganic Research.

(1) (a) McHugh, M. M.; Beerman, T. A.; Burhans, W. C. *Biochemistry* **1997**, *36*, 1003−1009. (b) Hu, J.; Xue, Y.-C.; Xie, M.-Y.; Zhang, R.; Otani, T.; Yamada, Y.; Marunaka, T. *J. Antibiot.* (*Tokyo*) **1988**, *41*, 1575−1579. (c) Zhen, Y.-S.; Ming, X.-Y.; Yu, B.; Otani, T.; Saito, H.; Yamada, Y. *J. Antibiot.* (*Tokyo*) **1989**, *42*, 1294−1298.

(2) (a) Okuno, Y.; Otsuka, M.; Sugiura, Y. *J. Med. Chem.* **1994**, *37*, 2266−2273. (b) Otani, T.; Minami, Y.; Marunaka, T.; Zhang, R.; Xie, M.-Y. *J. Antibiot.* (*Tokyo*) **1988**, *41*, 1580−1585.

(3) Matsumoto, T.; Okuno, Y.; Sugiura, Y. *Biochem. Biophys. Res. Commun.* **1993**, *195*, 659−666.

(4) Kappen, L. S.; Goldberg, I. H. *Science* **1993**, *261*, 1319−1321.

(5) (a) Xu, J.; Wu, J.; Dedon P. C. *Biochemistry* **1998**, *37*, 1890−1897. (b) Kumar, R. A.; Ikemoto, N.; Patel, D. J. *J. Mol. Biol.* **1997**, *265*, 173−186.

(6) Kumar, R. A.; Ikemoto, N.; Patel, D. J. *J. Mol. Biol.* **1997**, *265*, 187−201.

(7) Zein, N.; Colson, K. L.; Leet, J. E.; Schroeder, D. R.; Solomon, W.; Doyle, T. W.; Casazza, A. M. *Proc. Natl. Acad. Sci. U.S.A.* **1993**, *90*, 2822−2826.

(8) Okuno, Y.; Iwashita, T.; Otani, T.; Sugiura, Y. *J. Am. Chem. Soc.* **1996**, *118*, 4729−4730.

(9) Sugiura, Y.; Matsumoto, T. *Biochemistry* **1993**, *32*, 5548−5553.

(10) (a) McHugh, M. M.; Woynarowski, J. M.; Gawron, L. S.; Otani, T.; Beerman, T. A. *Biochemistry* **1995**, *34*, 1805−1814. (b) Cobuzzi, R. J.; Kotsopoulos, S. K.; Otani, T.; Beerman, T. A. *Biochemistry* **1995**, *34*, 583−592.

(11) Xu, Y. J.; Zhen, Y. S.; Goldberg, I. H. *Biochemistry* **1994**, *33*, 5947−5954.

(12) Iida, K.; Hirama, M. *J. Am. Chem. Soc.* **1995**, *117*, 8875−8876.

10.1021/ja994323a CCC: $19.00
Published on Web 07/08/2000

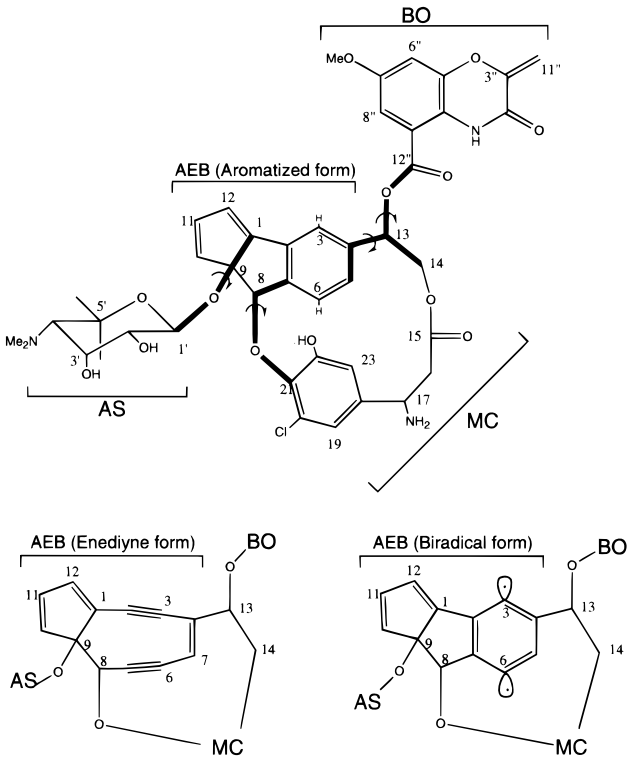

Figure 1. Chemical structures of aromatized (upper), enediyne (lower left), and 3,6-biradical (lower right) forms of C1027−Chr. The arrows show the characteristic dihedral angles shown in Table 2.

Chr, which structurally resembles the reactive biradical intermediate, was used in the NMR study, because the enediyne Chr easily undergoes cycloaromatization without a reductant and cleaves DNA in the course of NMR measurements (Figure 1). A heptamer d(T1G2C3C4A5T6C7)/d(G8A9T10G11G12C13A14) was chosen as the DNA substrate, and indeed the DNA oligomer contains a (5′-GCCAT/3′-ATGGC) recognition and cleavage site of C1027−Chr (cleaved residues underlined).[11]

NMR Experiments. Spectra were acquired on 600 MHz-JEOL and 750 MHz-Bruker spectrometers. Initial titration experiments monitored by one-dimensional (1D) NMR spectra confirmed a 1:1 complex formation on mixing of the DNA heptamer with C1027−Chr at 288 K in H_2O (30 mM NaCl, pH 7.0). The NOESY spectra (150 and 200 ms mixing times) of the complex in H_2O (30 mM NaCl, pH 7.0) were recorded at 288 K using the WATERGATE pulse sequence.[14] The NOESY spectra (100, 150, and 200 ms mixing times), TOCSY spectra (80 ms spin-lock time), and DQF-COSY spectra of the complex were obtained in D_2O (30 mM NaCl, pD 7.0) at 295 K. The ROESY spectra (80, 100, and 150 ms mixing times) of free Chr were also recorded in D_2O (pD 6.8) at 295 K, because stronger peaks of free Chr with a molecular mass of 845.5 Da were detected with ROESY rather than with NOESY. The resonances were assigned by established procedures.[15]

NOE-Derived Distance-Restraint Molecular Dynamics Simulations. Total NOE peaks in DNA−Chr complex and ROEs in free Chr were converted to distance restraints by the two-spin approximation. The offset dependence of the ROEs was taken into account on the basis of an established method.[16] Upper bounds added to the estimated distances were +0.5 Å for the DNA−Chr complex and +0.1 Å for free Chr. The minimum interproton distance limit was set to 1.8 Å for both the complex and free Chr. Distances to methyl protons were assigned to a pseudoatom at the geometrical center of these atoms, and a 0.5 Å correction was added to the upper bound. Interstrand hydrogen bonds were used as 18 restraints with force constants of 60 kcal/mol Å^2 to maintain Watson−Crick base pairing. All molecular simulations were performed using the XPLOR program. Initial starting structures, free Chr and DNA−Chr docking models, were generated using Quanta. The electronic and structural calculations on the Chr were performed with the program MOPAC. The starting structures were subjected to 500 steps of conjugate gradient energy minimization. Dynamics calculations were started at 10 K with heating to 1000 K over 5 ps. The NOE or ROE restraints were introduced gradually over 6 ps during the dynamics at 1000 K with the force constant for restraints increased from 2.0 to 30.0 kcal/mol Å^2. The introduced force constant was then maintained constant throughout the subsequent dynamics calculations. The system was maintained at 1000 K for 10 ps, gradually cooled to 300 K over 7 ps, and maintained at 300 K for 20 ps. Coordinates were stored every 0.5 ps for the last 4 ps and averaged. The obtained structures were then subjected to 2000 steps of Powell energy minimization.

Ab Initio Calculations and Singlet−Triplet Splitting. We used the biradical−aromatic ring systems consisting of the optimized *p*-benzyne-type biradical and benzene, which were superposed with biradical and chlorophenol rings of C1027−Chr in two (DNA and Apo) states. Optimized geometries of benzene and a *p*-benzyne-type biradical were obtained from density functional theory (DFT) using BPW91. Zero-point vibrational energies (ZPE) for each system were computed from the scaling factor (0.993). Singlet-point energy calculations (E_{tot}) were also carried out with BPW91/cc-pVTZ and CCSD(T)/cc-pVTZ. The singlet−triplet energy gap ΔE_{st} is defined according to (eq 1)

$$\Delta E_{st} = (E_{tot} + \mathrm{ZPE})\mathrm{triplet} - (E_{tot} + \mathrm{ZPE})\mathrm{singlet} \qquad (1)$$

These calculations were performed with GAUSSIAN94.

Results and Discussion

NMR Spectral Analysis of DNA−Chr Complex. The imino proton spectral region of free DNA duplex and the one drug per duplex complex exhibited well-resolved resonances consistent with formation of a predominant single conformation of the Chr−DNA complex (Supporting Information, Figure 1). The through space and through bond analysis of the two-dimensional data sets in H_2O and D_2O solution yielded almost complete lists of proton chemical shifts of the Chr−DNA complex (Supporting Information, Figure 2).

NOESY spectra of the complex showed the disruption of the sequential connectivities of the base and sugar (H2′ and H2″) protons at the (C3G12)-(C4G11) step (Supporting Information Figure 3). Upon admixture of Chr and DNA heptamer, we also detected upfield shifting of the benzoxazolinate (BO) protons (H6″, H8″, H11″, and methoxy-H) and the base-paired G11 and G12 imino protons (Figure 2 and Supporting Information Figures 1 and 2). These observation is consistent with intercalation of the BO ring at the (C3G12-C4G11) step.[17] Furthermore, the proton chemical shift perturbation of the heptamer and intermolecular NOEs by the formation of the DNA−Chr complex defined the relative alignment of the drug in DNA minor groove (Supporting Information Figures 2 and 4).

Solution Structures of DNA−Chr Complex, Apo−Chr Complex, and Free Chr. We clarified the solution structures of free Chr and the complex formed between the drug and a DNA oligomer by NMR techniques. The NOESY measurements of the Chr−DNA oligomer complex yielded a total of 144 DNA intramolecular, 33 drug intramolecular, and 36 DNA−drug intermolecular NOEs (Supporting Information Figure 4) that we were able to clearly assign. Free Chr in a D_2O solution provided 14 intramolecular ROEs in the ROESY (Supporting

(13) Iida, K.; Fukuda, S.; Tanaka, T.; Hirama, M.; Imajo, S.; Ishiguro, M.; Yoshida, K.; Otani, T. *Tetrahedron Lett.* **1996**, *37*, 4997−5000.

(14) Piotto, M.; Sandek, V.; Sklenar, V. *J. Biomol. NMR* **1992**, *2*, 661−665.

(15) Wuthrich, K., *NMR of Proteins and Nucleic Acids*; Wiley: New York, 1986.

(16) Kessler, H.; Bats, J. W.; Griesinger, C.; Koll, S.; Will, M.; Wagner, K. *J. Am. Chem. Soc.* **1988**, *110*, 1033−1049.

(17) Yu, L.; Mah, S.; Otani, T.; Dedon, P. *J. Am. Chem. Soc.* **1995**, *117*, 8877−8878.

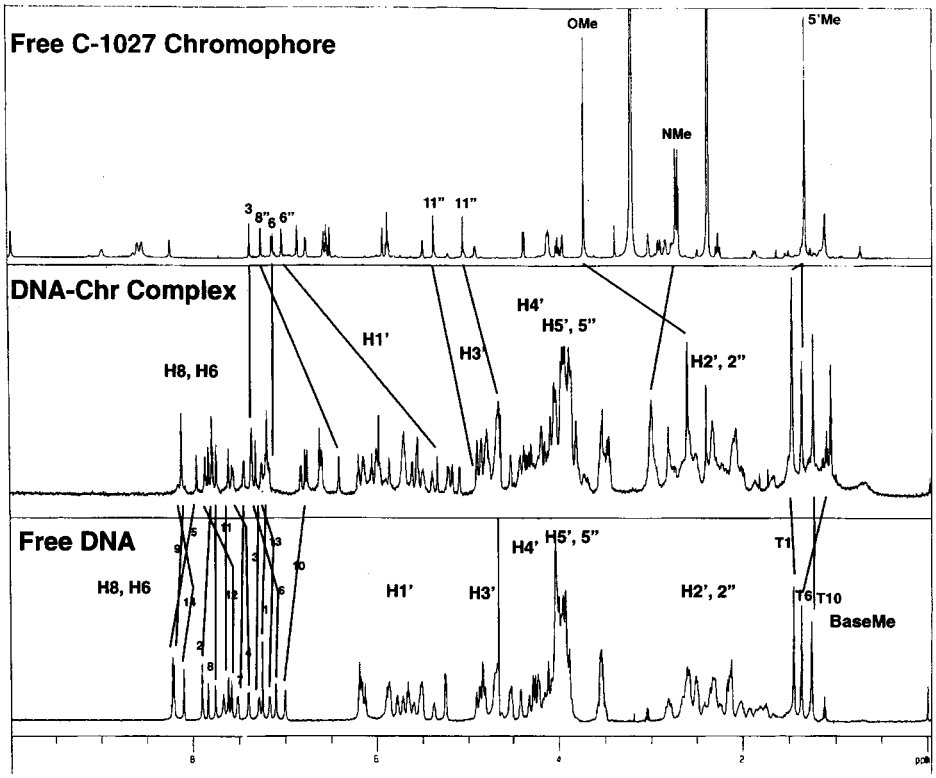

Figure 2. 1D ^{1}H NMR spectra for the free C1027−Chr (upper), the Chr−d(T1G2C3C4A5T6C7)/d(G8A9T10G11G12C13A14) complex (middle), and the free DNA heptamer (lower). The lines show chemical shift perturbations of the aromatic protons of the Chr and the DNA oligomer.

Information Figure 5). The solution structures of the DNA−Chr complex and free Chr obtained with distance-restrained molecular dynamics computations gave relevant models that were fully consistent with the observed NMR-derived distance data (Supporting Information Figure 6). In the unbound state, restrained molecular dynamics simulation illustrated that free Chr cannot fix its benzoxazolinate (BO) and aminosugar (AS) moieties in one specific conformation without characteristic interaction. Indeed, ROEs of the BO and AS parts were rarely detected. Because most of the observed intra-ROEs of Chr arose from the 16-membered macrocyclic part (MC), the conformation of MC was well-defined (Supporting Information Figure 5). Average pairwise rms deviations among the final structures were 0.72 Å for the DNA−Chr complex and 0.77 Å for free Chr. The generated structures of the DNA−Chr complex and free Chr were averaged and energy-minimized. To understand the molecular basis for the unique biological activity of C-1027, three-dimensional structures of the DNA−Chr complex, Apo−Chr complex, and free Chr are essential. Figure 3 indicates these solution structures for DNA−Chr complex, Apo−Chr complex,[18] and free Chr.

Chr−DNA Recognition. In the Chr−DNA heptamer complex (Figure 4A), the inter-NOEs of the BO and AS moieties with DNA were in the majority (75%) of all observed intermolecular peaks (Supporting Information Figure 4). The proton chemical shift perturbations of these functional moieties were also larger upon binding to DNA (Supporting Information Figure 2). Thus, both the BO and AS parts play important roles in the recognition and binding of Chr to DNA. The DNA−Chr complex model evidently revealed that C1027−Chr interacts with each tetranucleotide of the d(C3C4A5T6)/d(A9T10G11G12) duplex through unique intercalation of the BO moiety at the d(C3C4)/d(G11G12) step and also minor groove binding of the AS part at d(A5T6)/d(A9T10G11).

This complex is stabilized by the stacking interaction through intercalation and by the van der Waals interactions and a hydrogen bond interaction through the backbone helical and minor groove contacts. The intercalation of the BO moiety was demonstrated by the NOEs connecting 1″-NH with H6, H1′, H2′, 2″ of C3 and H6, NH_2 of C4; OMe with H8, H1, H1′ of G11; H6″ with H3′ of G12. One of the two six-membered rings of BO (the ring containing 1″-NH) stacks partially on the pyrimidine rings of C3 and C4, while the one containing a methoxy group stacks on the purine rings of G11 and G12. The protruding methoxy group of the BO moiety undergoes van der Waals contacts with H1′ of the G11 sugar.

Furthermore, the inter-NOEs of the AS moiety with the DNA oligomer were observed connecting β-Hs(H2′, H3′, H4′, and 6′-Meβ) with H1′ and H4′ of T6 and H2 of A5; α-Hs(4′-NMe and 6′-Meα) with H2 of A9, H1′ and H4′ of T10, and H4′, H5′, and H5″ of G11. There are backbone helical contacts between the AS part on one side and the helical sugar−phosphate backbones of A5T6 and A9T10G11 strands on the other side. The orientation of the AS moiety permits its α^1Hs and β^1Hs to face the A9T10-strand adn A5T6-strand, respectively. Another set of contacts was also detected between AS and the DNA minor groove floor. These contacts include the van der Waals interaction of AS H3′ and 4′-NMe with DNA A5(H2) and A9(H2) and a hydrogen bond of the AS 2′-OH with G11 2-NH_2 (Figure 4A1). This hydrogen bond supports our previous data that the guanine 2-amino group of the central base in trinucleotide 5′-AGG plays a key role in the recognition of the DNA oligomer by Chr.[19]

In addition, the observation of several NOEs showed the backbone helical binding between the aromatized AEB ring (H5, H6, and H8) and the DNA backbone [C4(H1′), A5(H1′ and H4′), and T6(H5′)] (Figure 4A2). An intermolecular NOE cross-peak

(18) We used the structure coordinates of the Chr−Apo complex supplied by Dr. Ishiguro. The coodinates were derived for the aromatized Chr−Apo complex.

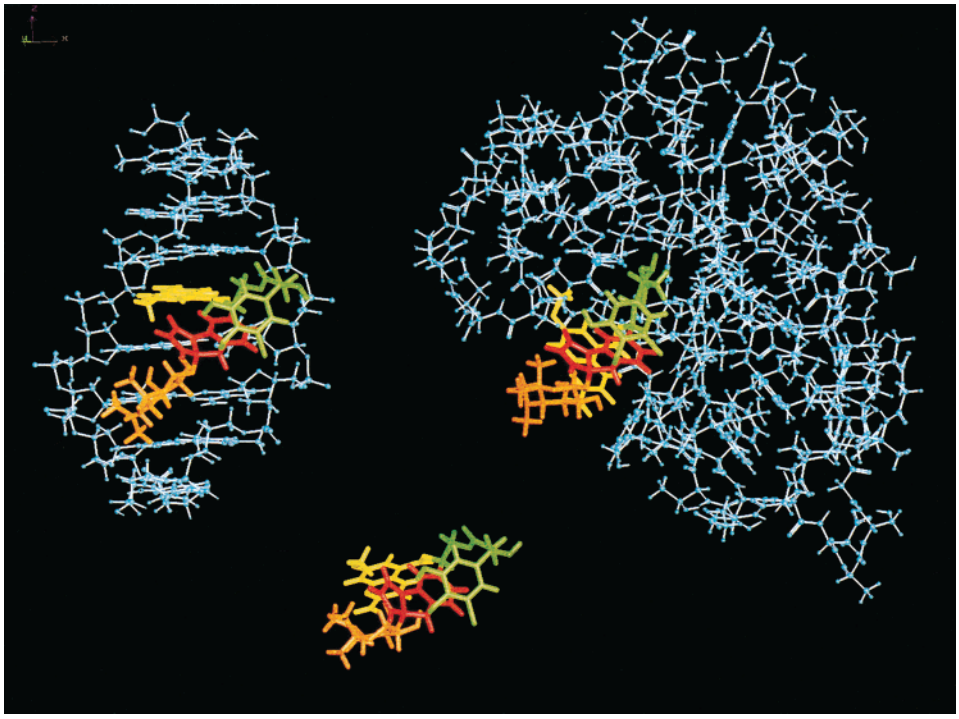

Figure 3. Solution structures of C1027−Chr−DNA heptamer complex (left), free Chr (center), and C1027−Chr−Apo complex (right). DNA and Apo are represented with light blue in ball-and-stick models. C1027−Chr consists of AEB (red), MC (green), BO (yellow), and AS (orange).

Table 1. Recognition Modes of Functional Moieties of C1027−Chr Bound to DNA and Apo

	To DNA	To Apo
benzoxazolinate	intercalation ($\pi-\pi$ stacking) at the d(C3C4)/d(G11G12) step	hydrophobic interaction with β-strand of the bottom of the pocket (van der Waals)
aminosugar	minor groove floor binding (hydrogen bond, van der Waals) backbone helical binding (van der Waals) with the d(A5T6)/d(A9T10G11)	no interaction covering over the pocket
macrocyclic ring	no interaction (hydrophobic int., hydrogen bond, salt-bridge)	bured and fixed at the bottom of the pocket
AEB	backbone helical binding with the d(C4A5T6) (van der Waals)	little interaction in the center of the hole (stacking interaction with Tyr32)

between Chr-H6 and A5-H1′ or −H4′ revealed the proximity of these protons. The Chr-H3 is situated close to H1′ of G12, as indicated by the constructed model. Therefore, it is reasonably proposed that the DNA lesions caused by the C-1027 Chr are due to the abstraction of hydrogen atoms from A5-C1′ or -C4′ by the Chr-C6 radical and from G12-C1′ by the Chr-C3 radical. In fact, our previous gel electrophoretic analysis evidently showed that the DNA damage occurs at CCA/TGG with a two nucleotide 3′-stagger of the cleaving residues. Thus, the intercalation of the BO spatially leads the reactive biradical atoms (C3 and C6) of the enediyne Chr to the vicinity of the deoxyribose hydrogen atoms (H1′ or H4′) of the DNA backbone (A5 and G12). The AS assists in winding of the Chr around the minor groove of the DNA oligomer. In contrast, the MC ring exhibited no clear interaction with DNA oligomer.

(19) Matsumoto, T.; Sugiura, Y. *Biochem. Biophys. Res. Commun.* **1994**, *205*, 1533−1538. In preliminary experiments of DNA−Chr titration, we tried various kinds of DNA oligomers containing GTTAT/ATAAC, CTTTT/AAAAG, ATAAT/ATTAT, CTTTA/TAAAG, and CTCTT/AAGAG. However, the imino proton-spectral region of complexes of Chrs with most oligomers except for d(TGCCATC)/d(GATGGCA) exhibited nonstoichiometric or broadening resonaces, indicating formation of multiple conformations of complex in each case. Namely, other duplexes except for d(TGCCATC)/d(GATGGCA) contain multiple binding sites despite single cleavage site by the Chr. The drug bound to a DNA sequence cannot always abstract the hydrogen atoms of the DNA nucleotides. Therefore, the 2-amino group of the central G is important to enhance specificity of DNA target recognition (not cleavage) by C1027−Chr.

Chr−Apo Recognition. The complex model of C-1027 (Figure 4B) demonstrates that the drug is packaged compactly by folding its BO and AS moieties in a hydrophobic pocket within Apo (Figure 4B1). The BO ring is located at the bottom of the pocket consisting of a β-strand (Tyr32-Ser52) and is covered by a β-turn (Ser74-Thr79). The MC ring also interacts with several residues at the bottom of the pocket. The As part scarcely contacts with Apo but covers the entrance of the binding pocket (Figure 4B2). In Apo, the AEB ring is sandwiched between the chlorophenol ring on one side and the BO and AS moieties on the other side (Figure 4B1). Moreover, some residues (Tyr32, Pro96, Ala95, and Asn97) constructing the pocket surround the AEB ring without specific contacts. Only a Tyr32 residue lies near the AEB ring and presumably contributes to the stabilization of Chr through a $\pi-\pi$ stacking interaction. Consequently, this reactive ring surrounded by the MC, BO, and AS moieties and these pocket residues, is protected from a hydrogen-attack.

Two Recognition Modes of Chr. Table 1 summarizes the recognition modes of Chr to DNA and Apo. The Chr mainly interacts with DNA through BO and AS moieties and with Apo through BO and MC moieties. The MC and AS parts hardly contribute to interactions with DNA and Apo, respectively.The AEB ring is parallel to the binding interface in DNA, while this is perpendicular in Apo. The AEB ring directly contacts

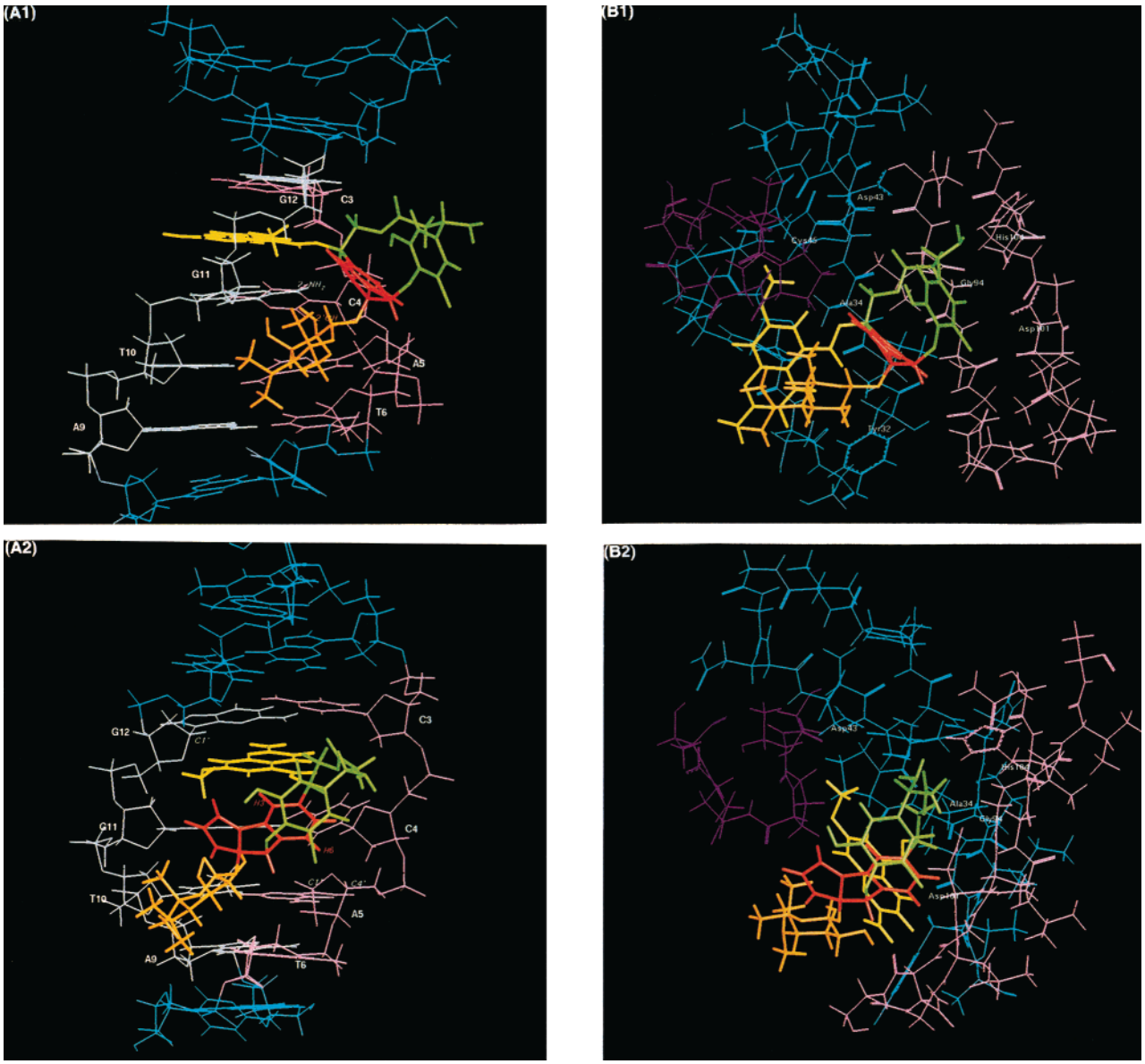

Figure 4. Drawing for binding sites of C1027−Chr with DNA heptamer (A) and C-1027 Apo (B). Side (A1 and B2) and front (A2 and B1) views of the binding interfaces. The AEB orientation of C1027−Chr in A1 and A2 is the same as that in B1 and B2, respectively. The strand d(C3C4A5T6)/d(A9T10G11G12) is colored in pink/light blue. Tyr32-Ser52, Ser74-Thr79, and Asn92-Ala106 residues composing the pocket of Apo are shown with blue, purple, and pink colors, respectively. The moieties of C-1027 Chr are colored as in Figure 2.

the minor groove of DNA, that is to say, but scarcely interacts with the pocket of Apo (Figure 4A2 and B1). Therefore, the guest (C1027−Chr) changes the direction of its hands [(BO and AS) or (BO and MC)] in response to the host (target DNA or carrier Apo) where Chr possesses two distinct interaction modes best fitted to the binding sites of the hosts. These conformational variations also reflect its function and reactivity. The enediyne part of Chr is situated in a position close to the target (deoxyribose) in DNA, whereas it is far from a hydrogen source in Apo.

Conformational Perturbation of Chr Dependent on Complex Formation and Increasing Temperature. Our previous work indicated that C-1027 is much more reactive in the presence of DNA than in its absence and that the drug is the most stable in Apo.[13] The reactivity of Chr decreases in the order of DNA-bound > free ≫ Apo-bound states. The structural comparison of Chrs in these three states would provide valuable insight into correlations between the conformation and the reactivity of C1027−Chr. The three average structures of Chrs bound to DNA and Apo[20] and free Chr were superimposed (Figure 5). As expected, the structural conformations of the BO and AS moieties in the three states were not superposed entirely (Figure 5A). The flexibility of the BO and AS moieties during the restrained molecular dynamics simulation of free Chr (Supporting Information Figure 6) suggests that the conformational perturbations of these moieties play no significant roles in regulating the reactivity of C-1027 Chr. Therefore, we investigated in detail the conformations of the 16-membered MC part containing a chlorophenol ring rather than those of the BO and AS moieties. Notably, a clear conformational deviation in the 16-membered MC part was observed between the DNA-bound and Apo-bound Chrs (Figure 5B). The MC moiety of the free Chr presents a conformation moderately

(20) Iida and Hirama reported that the constraint of the nine-membered ring of C1027−Chr may contribute to lowering the barrier for interconversion between the enediyne and biradical forms, and consequently the reaction process becomes reversible at ambient temperature. The hydrogen abstraction step by a biradical form is kinetically significant in the cycloaromatization of C1027−Chr. Therefore, the reactivity of C-1027 is affected more directly by conformation of aromatized form analogous to the biradical intermediate rather than by that of enediyne form.

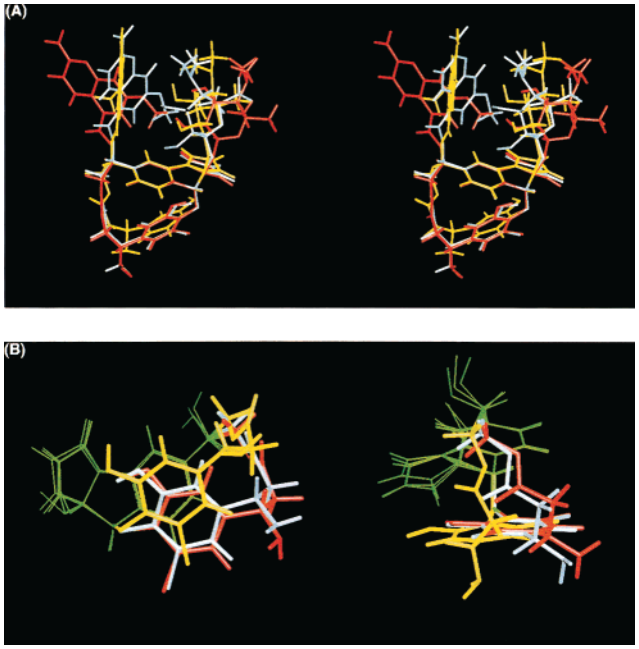

Figure 5. Superposition of C-1027 Chr bound to DNA (red) or Apo (yellow), and free Chr (light blue). The AEB moiety of Chr is superposed upon these three forms. A represents stereoview of the whole structures in these three states, and B indicates a conformational comparison of the MC moieties. Superposed AEB moieties are colored with green. The viewpoint on the left differs from that on the right in B.

Table 2. Characteristic Dihedral Angles (deg) of C1027−Chr Bound to DNA or Apo, and Free Chr

	In DNA	In Apo	free
	Benzoxazolinate		
(C4)(C13)(O)(C12″)	−136.4	67.84	−109.7
	Aminosugar		
(C1)(C9)(O)(C1′)	−50.55	−31.31	−10.29
	Macrocyclic ring		
(C5)(C4)(C13)(C14)	−79.41	−106.9	−89.40
(C7)(C8)(O)(C21)	−21.94	10.34	−15.75

similar to that of DNA-bound Chr. The dihedral angles [(C7)(C8)(O)(C21) and (C5)(C4)(C13)(C14)] of the linkage between the AEB and MC parts are respectively −21.94° and −79.41° in DNA and 10.34° and −106.9° in Apo. The deviation between the torsion angles in DNA and in Apo is 30 ± 2.5° (Table 2). This structural distinction arises from the difference between the interaction modes of the MC moiety with DNA and with Apo. The MC ring containing the chlorophenol is situated in the bottom of the pocket of the Apo. In addition, many interactions such as van der Waals contacts with Ala34, Gly94, and Cys36−45, the hydrogen bond of Chr-17NH_2 with His104, and salt-bridge between Chr-17NH_2 and residues Asp43 or Asp101 were detected (Figure 4B1). Especially, the intra-chlorophenol ring is pushed inside by the β-sheet wall (Asn92-Ala106) of the pocket, that is, steric hindrance (Figure 4B2). In contrast to that of the Apo-bound state, the MC part containing the phenol ring of Chr in the DNA-bound state did not exhibit distinct intermolecular NOEs, suggesting no clear interactions between this moiety and the DNA oligomer (Figure 4A1). Only one NOE peak between Chr (H16′) and DNA C4(H1′) indicates that the MC moiety is closer to the C4 strand, consistent with the values of the dihedral angle in DNA.

The previous experiments showed that the DNA cleavage reaction of C-1027 depends on temperature, namely increasing temperature promotes the reactivity of the drug.[9] To investigate the temperature-dependency of the conformation of Chr, we examined the 1D ^{1}H NMR spectra of free C1027−Chr at temperatures from 295 to 315 K. Only one proton (H23) of the chlorophenol ring shifted downfield with increasing temperature, though no other protons were field-shifted (Figure 6). The proton chemical shift of H23 is affected by the electric field of the nine-membered AEB ring, suggesting the existence of a subtle configurational perturbation of the chlorophenol ring with the rise in temperature.

Table 3. Computed Total Energies, Zero-point Energies, and S−T Splittings[a] for Biradical−Aromatic Ring Systems in Apo and DNA

	CCSD(T)/pVTZ	BPW91/pVTZ	ZPE
	In Apo		
triplet	−460.2375522	−463.2012796	107.0864691
singlet	−460.1084965	−463.1971597	105.7723144
S−T spilitting[b]	1.1850990	1.3100348	
	In DNA		
triplet	−460.2296099	−463.1959909	107.3332236
singlet	−460.0998565	−463.1911972	106.0589484
S−T spilitting	1.1445218	1.2694815	

[a] Total energies in au; zero-point energies and S−T splittings in kcal/mol. [b] S−T splitting = (E_{tot} + ZPE)triplet − (E_{tot} + ZPE)singlet.

These results led to our presumption that the conformational alteration of the MC part adjacent to the reactive AEB moiety closely relates to the reactivity of C-1027 Chr. In particular, the spatial configuration between the chlorophenol ring and AEB ring plays an important role in controlling the reactivity. The Chr retains an inactive conformation in Apo but becomes an active form in DNA.

Correlation between Reactivity and Conformation of Chr. We evaluated the influence of spatial configuration of the neighboring aromatic ring on the reactivity of the biradical by an ab initio method.[21] Recently, Chen and co-workers pointed out that the reactivity of *p*-benzyne type biradicals depends on the energy splitting between the singlet (S) ground state and the triplet (T) excited state; the larger the S−T splitting becomes, the less reactive is the singlet biradical.[22] On the basis of this information, we estimated and compared the S−T splittings of both biradical-aromatic ring systems that are conformationally similar to C1027−Chrs in DNA and Apo. The S−T splitting of the biradical-aromatic ring system in DNA was slightly smaller than that in Apo (Table 3). Accordingly, the *p*-benzyne type biradical in DNA is more reactive than that in Apo, because of the conformational alteration of the MC part containing a chlorophenol ring.[23] It is possible for the drug to control the reactivity of hydrogen-abstraction reactions by subtle structural perturbation of the intramolecular chlorophenol ring adjacent to the reacting AEB system.[24] On the other hand, neocarzinostatin (NCS), esperamicin, calcheamicin, and kedarcidin require an external cofactor (thiol) as a trigger for the Bergmann reaction.

(21) (a) Cramer, C. J.; Squires, R. R. *J. Phys. Chem.* **1997**, *A101*, 9191−9194. (b) Cramer, C. J.; Nash, J. J.; Squires, R. R. *Chem. Phys. Lett.* **1997**, *277*, 311−320.

(22) Logan, C. F.; Chen, P. *J. Am. Chem. Soc.* **1996**, *118*, 2113-2114.

(23) We used the benzene ring as a group adjcent to p-benzyne biradical for the purpose of the simplicity of ab initio calculation. If chlorophenol ring is employed instead of benzen ring, the functional substituent groups (chloro- and hydroxyl-group) may influence the magnitude of S−T splitting difference for the two C1027−Chr form. Therefore, the calculated S−T gap difference (∼0.04) can indicate qualitative tendency of the C1027-reactivity. More accurate calculations will lead to these quantitative interpretations.

(24) (a) Stassinopoulos, A.; Ji, J.; Gao, X.; Goldberg, I. H. *Science* **1996**, *272*, 1943−1946. (b) Gao, X.; Stassinopoulos, A.; Rice, J. S.; Goldberg, I. H. *Biochemistry* **1995**, *34*, 40−49. (c) Kim, K.-H.; Kwon, B.-H.; Myers, A. G.; Rees, D. C. *Science* **1993**, *262*, 1042−1046.

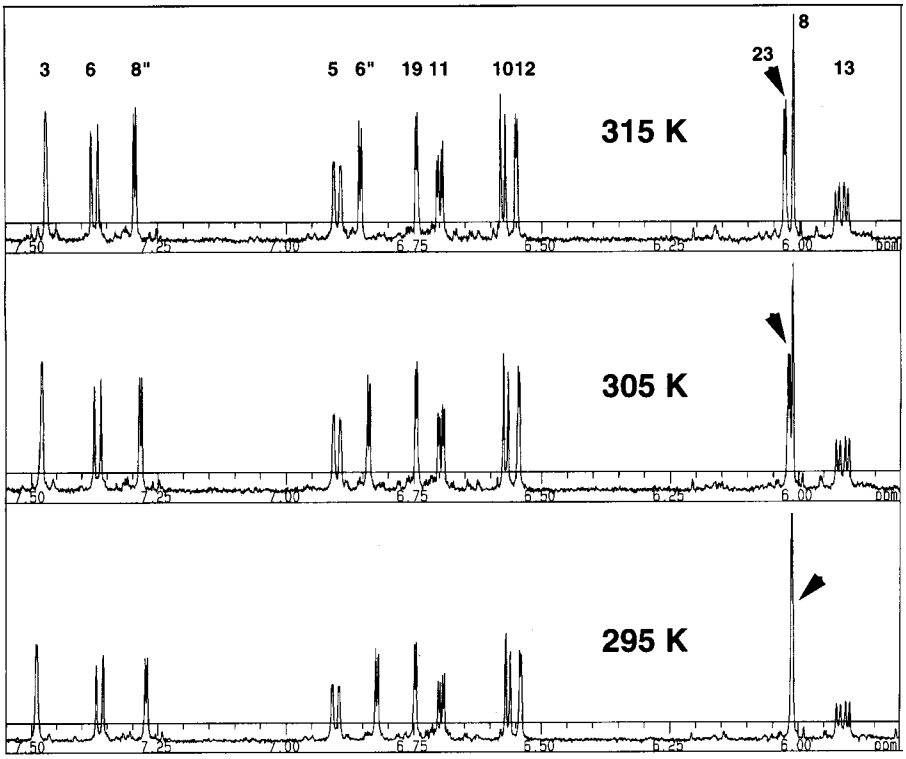

Figure 6. 1D ^{1}H NMR spectra (5.8−7.55 ppm) of free Chr at different temperatures from 295 to 315 K. The arrows show H23 proton chemical shift perturbation.

Conclusions

A reasonable mechanism for the different reactivity of C-1027 is proposed on the basis of structural considerations. In Apo, C1027−Chr is tacitly stabilized by four factors: (1) remote positioning from a hydrogen source in the pocket of Apo, (2) π-stacking interaction between the AEB rings and Tyr32, (3) protection of the AEB moiety by sandwiching it among the intra-chlorophenol ring to the biradical ring by constraint of the 16-membered MC moiety in the pocket. The free Chr released from Apo decreases in stability and then is converted into a reactive form because of removal of the conformational constraints of the MC part in Apo. By binding to DNA, the Chr relaxes the BO and AS moieties which were folded in Apo, and exposes its enediyne biradical ring to the DNA minor groove. Simultaneously, the biradical species is accessible to the hydrogen atoms of the DNA nucleotides and enhances the hydrogen abstraction kinetics, followed by DNA damage. Although the structures of NCS−Chr complexes with DNA and Apo have been previously determined by NMR and X-ray methods,[13,24c] the structural comparison of both the complexes and the structure−reactivity relation of NCS have never been established. In contrast with the reaction of NCS−Chr triggered by thiol, C1027−Chr is a very interesting model of DDS. The present evidence provides the first molecular basis of a natural DDS. We can understand how C-1027 recognizes the carrier (Apo) and the target (DNA) and how its reactivity is controlled in both hosts.

Acknowledgment. We thank Dr. M. Ishiguro for providing the refined coordinates of the Apo−Chr complex. This study was supported in part by a Grant-in-Aid for Scientific Research (10771317) from the Ministry of Education, Science, Sport, and Culture, Japan. Computation time was provided by the Supercomputer Laboratory, Institute for Chemical Research, Kyoto University.

Supporting Information Available: NMR spectral data and molecular dynamics structures of the DNA−Chr complex and free Chr (PDF). This material is available free of charge via the Internet at http://pub.acs.org.

JA994323A